LBL-12878
UC-21

Lawrence Berkeley Laboratory
UNIVERSITY OF CALIFORNIA

Accelerator & Fusion Research Division

THE RESISTIVE WALL INSTABILITY IN A UNIFORM BEAM: SIMULATION VS. ANALYTICAL RESULTS

Abraham Sternlieb

June 1981

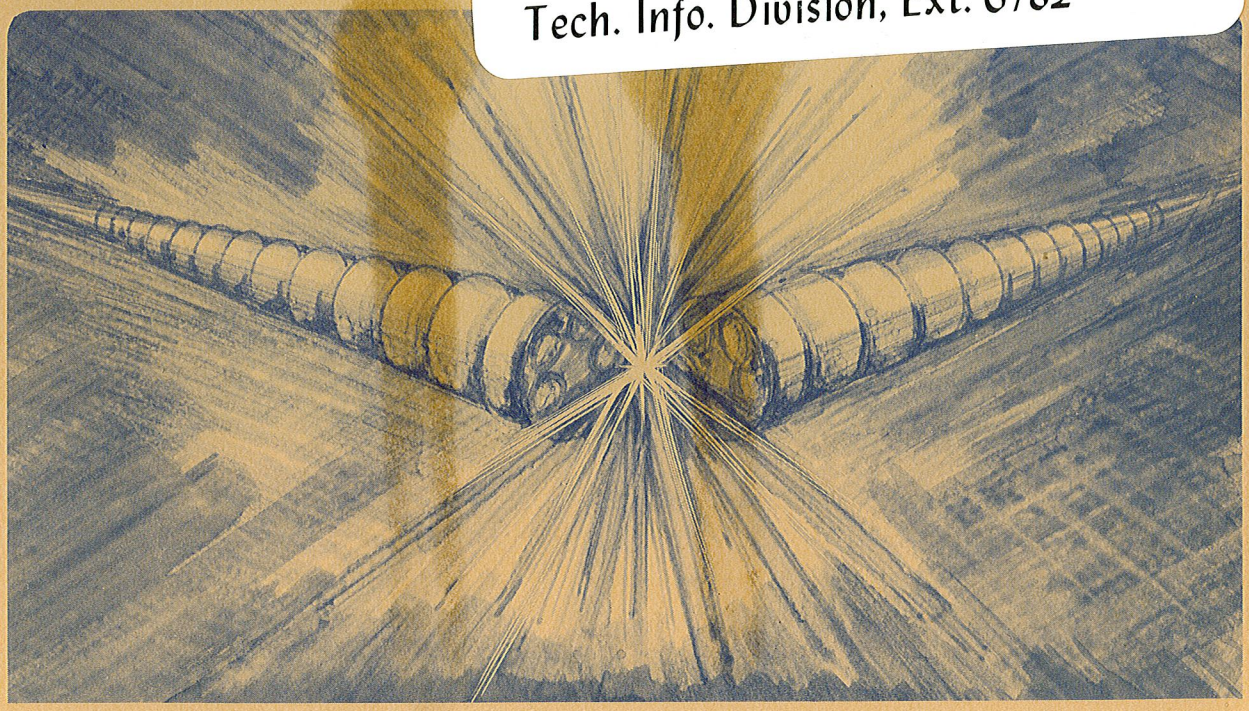

Prepared for the U.S. Department of Energy under Contract W-7405-ENG-48

LBL-12878

THE RESISTIVE WALL INSTABILITY IN A UNIFORM BEAM: SIMULATION VS. ANALYTICAL RESULTS

Abraham Sternlieb

Lawrence Berkeley Laboratory
University of California
Berkeley, California 94720

June 1981

*This work was supported by the Director, Office of Energy Research, Office of Inertial Fusion, Research Division of the U.S. Department of Energy under Contract No. W-7405-ENG-48.

The figures were printed from originals provided by the author.

The Resistive Wall Instability in a Uniform Beam: Simulation vs. Analytical Results

A. Sternlieb

Lawrence Berkeley Laboratory
University of California
Berkeley, California 94720

ABSTRACT

The time-dependent behavior of the resistive wall instability in a uniform charged beam is investigated by means of computer simulation. Results are compared with linear analytical results for a range of cases in which two parameters are varied: the resistive wall term and the initial thermal spread of the beam. In general we find good agreement between simulation and theoretical results. The main conclusion is that the growth rate of any mode increases with the resistive term and decreases as a function of the thermal spread. There is always a maximum marginally unstable wavenumber k for any nonzero thermal spread. The linear growth rate is roughly the same for the thermal spread and for the electric field amplitude. An "overshoot" phenomenon is present, in the sense that the thermal spread continues to grow after the electric field has reached saturation.

I. INTRODUCTION

A cold uniform beam with space-charge is unstable against perturbations if a resistive wall force is present. However, a non-zero thermal spread in the beam has a stabilizing effect, quenching the growth of all wavelengths shorter than a certain limiting value. This limiting wavelength (or correspondingly, wavenumber) is a function of: (a) R'-wall resistance per unit length, (b) v_{th}-thermal spread, (c) other physical parameters like: v_B-the beam velocity, n-number of particles per unit length, q-charge per particle, m-mass of particle, g-geometric factor related to pipe and beam radii.

It is the purpose of this report to study the above phenomena by means of

computer simulation and to compare to known anlytical results[1]. The theoretical analysis used is linear, providing a dispersion relation for the complex frequency as function of the system parameters. The simulation code[2] follows the motion of thousands of particles under the influence of self-consistent space-charge and external forces. In the simulations, the complex frequency is found from the time dependence of the fourier components of the electric field. The advantages of the computer simulation is that it shows clearly both the linear and the non-linear saturation regime. In the uniform beam case the focusing force is turned off. The initial velocity distribution is either cold or gaussian. The density distribution is randomly uniform.

The purpose of this report is to provide a preliminary basis for the study of bunched beams, where coasting beam results will be used as first estimates for initial guidance in interpreting simulation results.

In section II we present a short summary of the linear theory, including thermal spread. In section III we present simulation results for various cases and compare with analytical results. In section IV we draw some general conclusions.

II. LINEAR THEORY OF RESISTIVE INSTABILITY IN UNIFORM BEAMS

We assume complete decoupling between the longitudinal and transverse dimensions. Then, by using the long wavelength formula for the electric field and linearizing the 1-d Vlasov equation for the longitudinal dimension, we obtain:

$$1 = -\frac{q^2}{m}(kg + iR)\int \frac{(\partial f_0/\partial v)dv}{\omega - kv} \quad , \qquad (1)$$

where q is the ion charge, m is the ion mass, k is the wavenumber, g is a geometric factor, $R = R'v_B$ where R' is the resistance per unit length and v_B is beam velocity; $f_0(x,v)$ is the stationary distribution function and ω is the complex frequency: $\omega = \omega_R + i\gamma_k$.

Let us take for $f_o(x,v)$ in eq. (1) a gaussian distribution:

$$f_o(x,v) = \frac{n_o}{(2\pi)^{1/2} v_{th}} \cdot e^{-v^2/2v_{th}^2} \quad , \tag{2}$$

where n_o is the number density and v_{th} is the thermal spread. Then we obtain:

$$1 = \frac{k v_p^{\,2}}{(2\pi)^{1/2} v_{th}} (k + i \frac{R}{g}) \int_{-\infty}^{+\infty} \frac{e^{-v^2/2v_{th}^2}}{(\omega - kv)^2} \, dv \quad , \tag{3}$$

where v_p is a characteristic phase velocity in the system defined by:

$$v_p = \sqrt{\frac{n_o q^2 g}{m}} \tag{4}$$

Eq. (8) is the accurate linear dispersion relation for a uniform beam with a gaussian velocity distribution, giving ω_R and γ_k as functions of k, for a given set of physical parameters: R, v_{th}, v_p.

For a cold beam $v_{th} \to 0$, $f_o(x,v)$ in eq. (2) becomes a δ-function, and eq. (3) becomes:

$$\omega^2 = v_p^{\,2} k^2 (1 + i \frac{R}{kg}) \tag{5}$$

Eq. (5) has as a solution two opposedly propagating waves, the forward one damping and the backward one growing. In the case of a small resistive term,

$$\frac{R}{kg} \lesssim 1 \tag{6}$$

and we obtain:

$$\left.\begin{aligned} \omega_R &= \pm v_p \cdot k \\ \gamma_k &= + \frac{1}{2} v_p \cdot \frac{R}{g} \end{aligned}\right\} \tag{7}$$

which is valid within less than 10% error for g = 1. The length of our system is 128 units, which gives a lowest wavenumber k_{min} of 0.049 $\left(k_{min} \equiv \frac{2\pi}{L_{system}}\right)$. Therefore in our cases eq. (7) is valid within less than 10% error for $R \lesssim 0.1$,

except for the first wave number $n = (k/k_{min}) = 1$ in the R = 0.1 case.

Exact solutions of eq. (5) (cold beam case) for R = 0.01, 0.1 and 1., and for the first 13 modes are presented in Table 1. Solutions of eq. (3) (warm beam case) are presented in Table 2 for $v_p = 13$, R = 0.1 and v_{th} ranging from 1 to 15. For convenience, these values are also displayed graphically in Figs. 1(a) and 1(b). Taking $\gamma_k = 0$, one obtains the values of the maximum unstable wavenumber k^{max}, as function of the thermal spread v_{th} (Fig. 1(c)). It is clear that the growth rates γ_k are only slightly affected for $v_{th} < 4$, but strongly diminished for $v_{th} > 4$. Practically all the modes are stabilized for $v_{th} \approx v_p$.

III. SIMULATION RESULTS

In this section we present simulation results for several values of the resistive term R and thermal spread v_{th}. These results are to be compared with the analytical results, eqs. (5) and (7) (cold beam case, Table 1) and eq. (3) (warm beam case, Table 2). The linear charge density is uniformly random, and the velocity distribution is gaussian. The phase velocity v_p is 13. The simulation system is fixed in the beam frame of reference. The space charge field is given by $-\partial\rho/\partial x$ and the resistive force by $-qR(\rho - \rho_o)$.

A. Cold Beam Case ($v_{th} = 0$)

Several values of R are considered. In Fig. 2(a) we present the evolution in time of the thermal spread. For R < 0.01 the growth rates are quite small. For R = 0.1 we have $\gamma_{v_{th}} \approx 0.6$, and for R = 1, $\gamma_{v_{th}} \approx 4$. A case with R = 0.1 but with only the seventh mode active starts slowly and eventually attains a growth rate $\gamma_{v_{th}} \approx 0.5$. These values should be compared with those in Fig. 2(b) where $E_x \equiv \sum_k |E_k|^2$ (E_k is the k-component of the electric field) is plotted as function of time for the various cases, giving "effective" growth rates which are similar to the corresponding values of $\gamma_{v_{th}}$ in Fig. 2(a), as expected.

An important feature to notice in comparing Figs. 2(a) and 2(b) is that the thermal spread continues to grow after the electric field has reached

saturation ("overshooting"). In Fig. 3 we have plotted the time evolution of the first four modes for R = 0.001. It is clear that the real frequency ω_R is proportional to k, $\omega_R = \alpha k$, with $\alpha \approx 12.8$. This compares well with the expected analytical results (eq. 7).

Our reference case is R = 0.1, which corresponds to a realistic set of physical parameters relevant to Heavy Ion Fusion. Simulation results are presented in Fig. 4. For most modes $\gamma_k \approx 0.6$, and $\gamma_1 \approx 0.5$. As a special case, we ran a simulation with the resistive term R = 0.1 acting only on the seventh mode (Fig. 5). As it can be seen, this is a nice way to determine accurately the linear growth rate of a specific mode, because it delays considerably the onset of the nonlinear saturation regime.

B. Warm Beam Case ($v_{th} \neq 0$)

We investigate several cases, all with the same resistive term R = 0.1, but with different initial thermal spreads. Because the initial electric field is determined solely by the initial charge distribution, it it the same as in the cold beam case with R = 0.1, and thus we are able to see the differential influence of an initial thermal spread on the subsequent evolution of the resistive instability. As a rule, we find that any nonzero initial thermal spread decreases the growth rates of the entire k-spectrum as compared to the cold beam case, with the suppression of all modes above a certain limiting value. A saturation of the thermal spread and electric field is attained in all cases, when particles and fields coexist in a steady state. In the final stages of the instabilities, only low wavenumbers still persist in the system.

As can be seen from Figs. 6 and 7, if $v_{th} < 4$ the growth rates are not significantly different from the cold case. It seems that a marked change in the stability properties occurs between $v_{th} = 4$ and 5. Cases with $v_{th} \geq 5$ are quite stable. This compares qualitatively well with the analytical results . The "overshoot" phenomenon is apparent here too, in the snese that the thermal spread continues to grow after the electric field has reached saturation. The behavior of the actual growth rate can be interpreted as a result of two opposing factors: (1) the growth because of the resistive term

and (2) the Landau damping because of the resonant interaction of $\frac{\omega_R}{k}$ waves with the tail of the velocity distribution function $f(v = \frac{\omega_R}{k})$.

Because of the difficulty in determining accurately growth rates, several warm beam cases will be discussed only qualitatively. In Fig. 8 it is apparent that for $v_{th} = 2$ the time evolution of the several modes displayed is very much similar to the cold beam case (with $R = 0.1$). In the cases with $v_{th} = 4$ and 5 (Figs. 9 and 10) growth rates for the lowest wavenumbers are not affected significantly, while growth rates of high modes are reduced considerably by the presence of the thermal spread. This is because the phase velocity $(\omega_R/k) > v_p$, and decreases toward v_p with increasing k (if $v_{th} \neq 0$), which affects correspondingly the Landau damping. Finally, for $v_{th} = 10$ (Fig. 11) most modes stay at constant level, on the average.

IV. CONCLUSIONS

We have performed particle computer simulations of the resistive wall instability in a nonnuetral continuous uniform beam. The agreement with the known analytical results, expecially in the cold beam case, is good, indicating that the simulation code can indeed provide an independent means for investigating this type of instability. All systems relax by thermalization towards a dynamic steady state in which the thermal spread and electric field eventually reach saturation (at different times).

ACKNOWLEDGEMENT

The author would like to thank Dr. Lloyd Smith and Joseph Bisognano for their useful discussions.

REFERENCES

1. A. G. Ruggiero and V. G. Vaccaro, "Solution of the Dispersion Relation for Longitudinal Stability of an Intense Coasting Beam in a Circular Accelerator", ISR-TH/68-33, Geneva, July 1st, 1968.

2. A. Sternlieb et al., LBL-12205, HI-FAN-144, January 1981.

Table 1: γ_k and ω_R/k for $v_{th} = 0$
(the upper values are ω_R/k; $k \approx 0.05n$)

n \ R	0.01	0.1	1
1	12.970 0.064	16.49 0.50	42.20 1.97
2	12.920 0.064	14.22 0.59	30.60 2.72
3	12.910 0.064	13.56 0.61	25.58 3.25
4	12.900 0.064	13.29 0.63	22.70 3.67
5	12.900 0.064	13.16 0.63	20.80 4.00
6	12.900 0.065	13.08 0.64	19.40 4.30
7	12.900 0.065	13.04 0.64	18.43 4.52
8	12.900 0.065	13.01 0.64	17.64 4.72
9	12.900 0.065	12.99 0.64	17.00 4.90
10	12.900 0.065	12.97 0.64	16.50 5.05
11	12.900 0.065	12.96 0.64	16.07 5.18
12	12.900 0.065	12.95 0.64	15.70 5.29
13	12.900 0.065	12.94 0.64	15.43 5.39

Table 2: γ_k for v_{th} = 1–15, n = 1–13 ($k \approx 0.05n$)

(v_p = 13, R = 0.1)

n \ v_{th}	1	2	3	4	5	6	7	8	9	10	11	12	13	14	15
1	.49	.49	.48	.48	.47	.46	.46	.45	.40	.38	.32	.18	.09	.03	
2	.55	.51	.48	.44	.41	.37	.30	.22	.11						
3	.58	.54	.51	.47	.44	.32	.14	.07							
4	.61	.58	.55	.52	.38	.23	.04								
5	.61	.58	.55	.52	.35	.18									
6	.62	.60	.58	.49	.30	.04					LINEARLY				
7	.61	.59	.56	.48	.27						STABLE				
8	.61	.58	.55	.46	.24						REGION				
9	.61	.58	.53	.45	.20						($\gamma_k \leq 0$)				
10	.61	.58	.55	.43	.15										
11	.61	.58	.55	.42	.10										
12	.61	.58	.56	.40	.05										
13	.61	.58	.56	.40	.01										

Figure Captions

Fig. 1: (a) γ_k as function of v_{th} for several k's; $v_p = 13$, $R = 0.1$

(b) γ_k as function of k for several values of v_{th} $(t = 0)$; $v_p = 13$, $R = 0.1$

(c) Marginal stability: k^{max} vs. v_{th}

Fig. 2: (a) v_{th} as function of time, for $v_p = 13$, v_{th} $(t = 0) = 0$ and $R = 0$, 0.001, 0.01, 0.1 and 1.

(b) $E_x^2 \equiv \sum_k |E_k|^2$ as function of time, for $v_p = 13$, v_{th} $(t = 0) = 0$, and several R - values.

Fig. 3: $E_k^2(t)$ for $R = 0.001$ and v_{th} $(t = 0) = 0$.

Fig. 4: $E_k^2(t)$ for $R = 0.1$ and v_{th} $(t = 0) = 0$.

Fig. 5: $E_k^2(t)$ for $R = 0.1$ and v_{th} $(t = 0) = 0$; only the 7th mode is active.

Fig. 6: $E_x^2(t)$ for $R = 0.1$ and several values of v_{th} $(t = 0)$; $E_x^2 \equiv \sum_k |E_k|^2$

Fig. 7: v_{th} (t) for $R = 0.1$ and several values of v_{th} $(t = 0)$.

Fig. 8: E_k^2 (t) for $R = 0.1$ and v_{th} $(t = 0) = 2$.

Fig. 9: E_k^2 (t) for R = 0.1 and v_{th} (t = 0) = 4.

Fig. 10: E_k^2 (t) for R = 0.1 and v_{th} (t = 0) = 5.

Fig. 11: E_k^2 (t) for R = 0.1 and v_{th} (t = 0) = 10.

FIG. 1(a)

$\nu_t = 13$, $R = 0.1$

$\gamma_k(\nu_{th})$

$k = 0.05n$

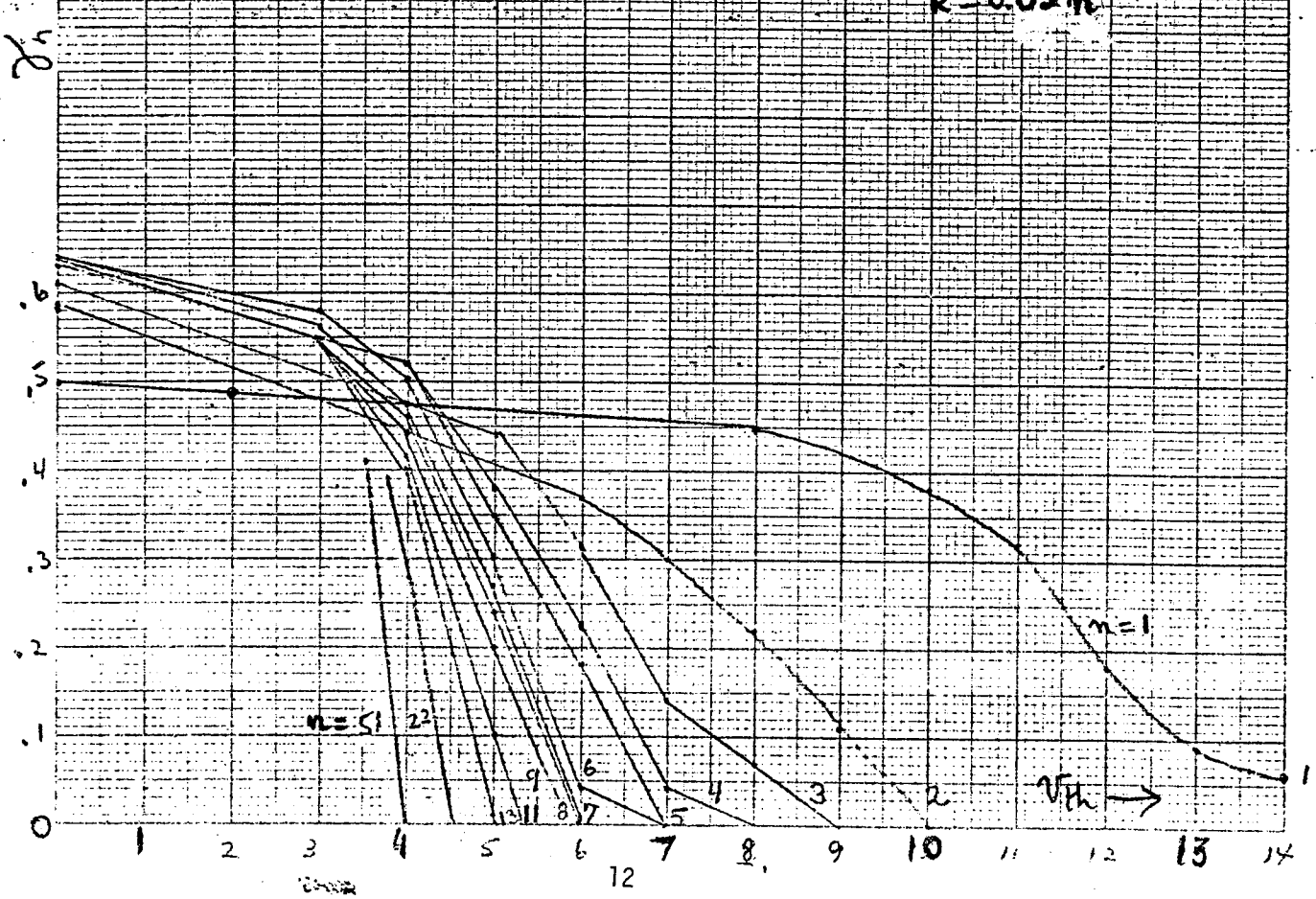

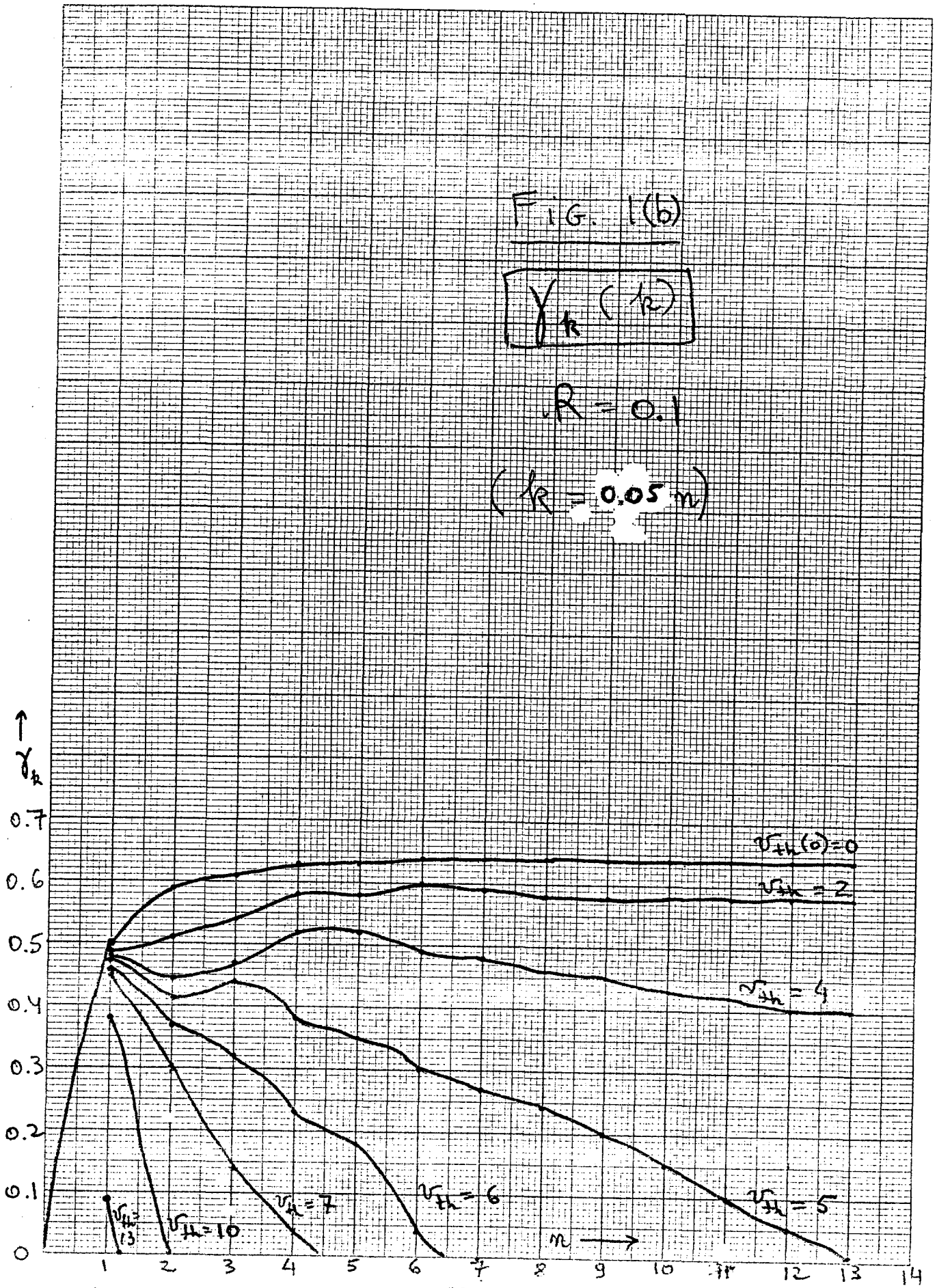
FIG. 1(b)
$\gamma_k(R)$
$R = 0.1$
($R = 0.05$ m)
γ_k
0.7
0.6
0.5
0.4
0.3
0.2
0.1
0
$v_{th}(0) = 0$
$v_{th} = 2$
$v_{th} = 4$
$v_{th} = 5$
$v_{th} = 6$
$v_{th} = 7$
$v_{th} = 10$
$v_{th} = 13$
m
1 2 3 4 5 6 7 8 9 10 11 12 13 14

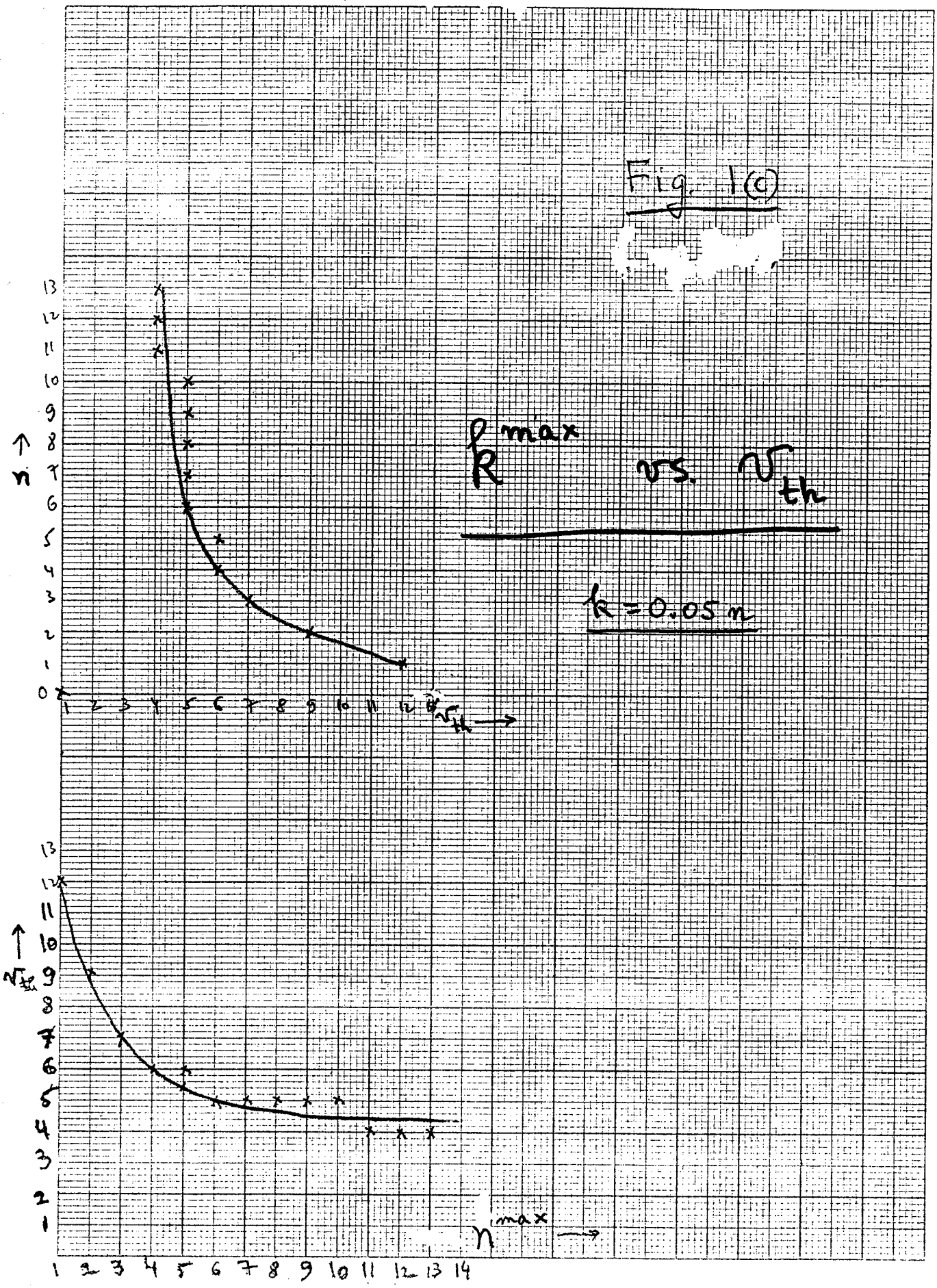
Fig. 1(c)
R_{max} vs. ν_{th}
$k = 0.05\ n$
n
ν_{th}
n_{max}
ν_{th}

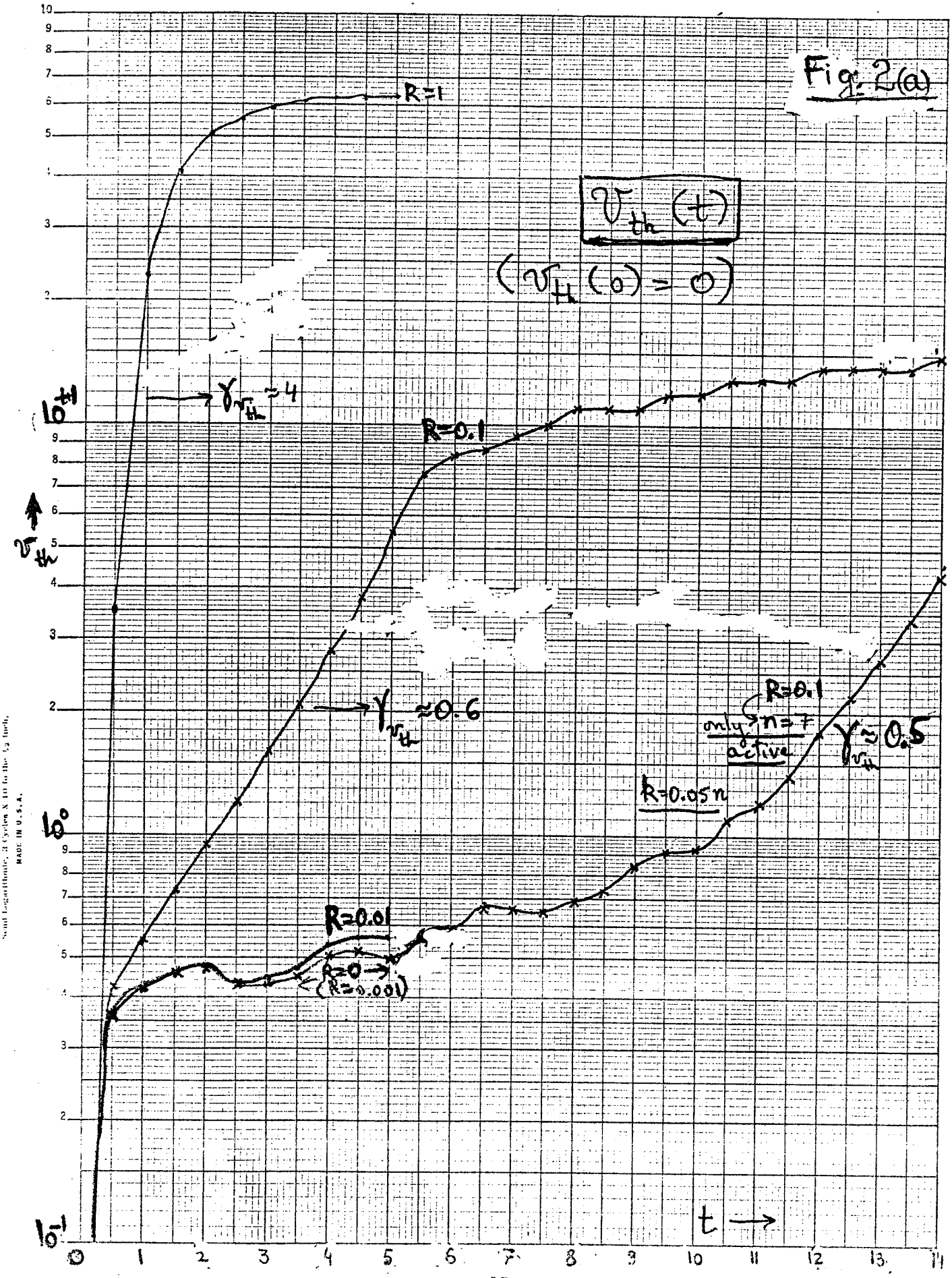
Fig. 2(a)
$v_{th}(t)$
$(v_{th}(0) = 0)$
R=1
R=0.1
R=0.01
R=0
(R=0.001)
R=0.05n
R=0.1
only n=1 active
$\gamma_{v_{th}} \approx 4$
$\gamma_{v_{th}} \approx 0.6$
$\gamma_{v_{th}} \approx 0.5$
v_{th}
$t \rightarrow$
10^{+1}
10^{0}
10^{-1}
0 1 2 3 4 5 6 7 8 9 10 11 12 13 14

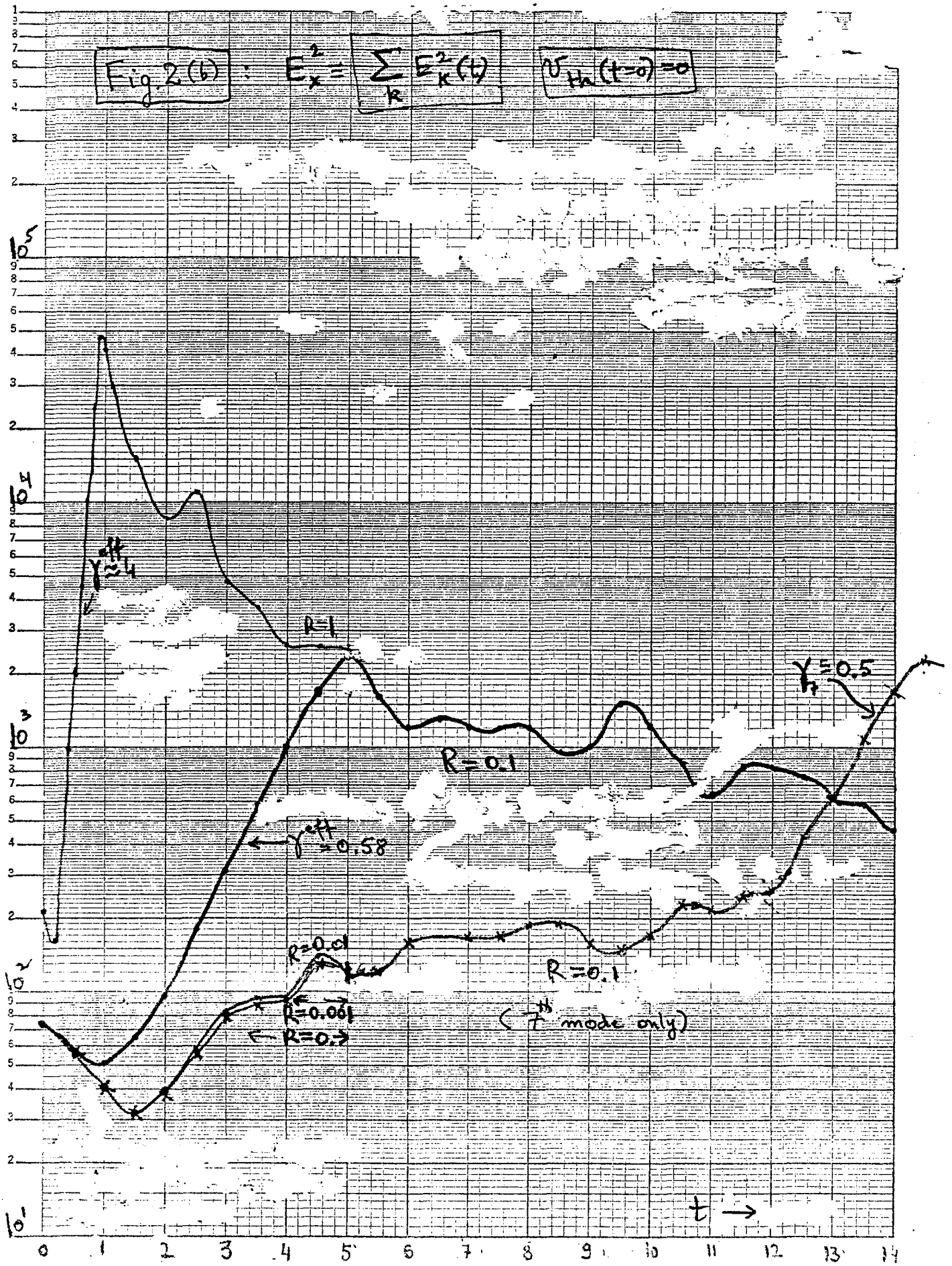
Fig. 2.(b) : $E_x^2 = \sum_k E_k^2(t)$
$v_{th}(t=0) = 0$
$\gamma^{th} \simeq 4$
R=1
R=0.1
$\gamma_1 = 0.5$
$\gamma^{th} = 0.58$
R=0.01
R=0.001
R=0.1
(1^{st} mode only)
10^5
10^4
10^3
10^2
10^1
t →
0 1 2 3 4 5 6 7 8 9 10 11 12 13 14

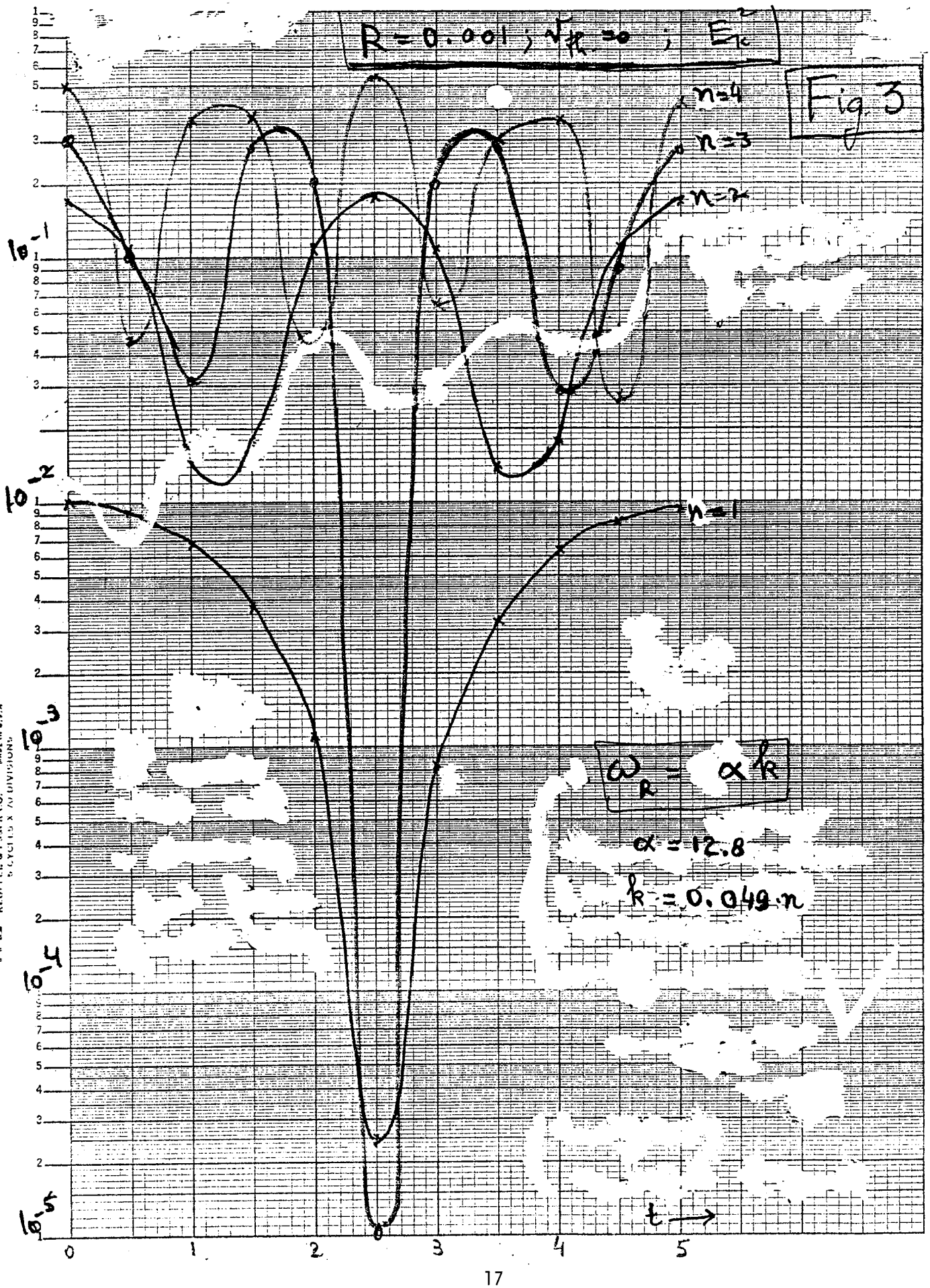
R = 0.001 ; $\nu_k = 0$; E_k^2
Fig. 3
n=4
n=3
n=2
n=1
10^{-1}
10^{-2}
10^{-3}
10^{-4}
10^{-5}
$\omega_R = \alpha k$
$\alpha = 12.8$
$k = 0.049 n$
t →
0
1
2
3
4
5

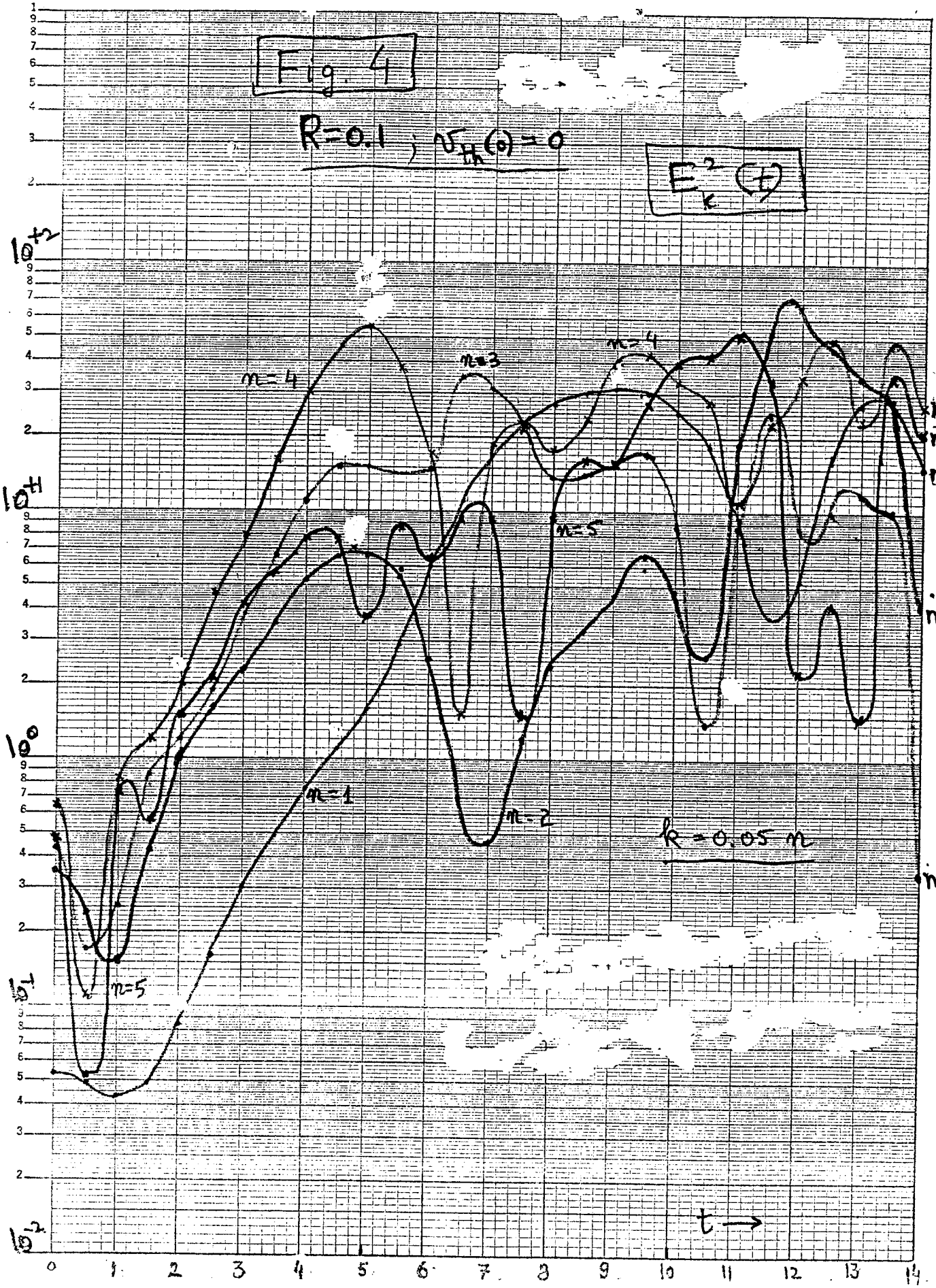
Fig. 4
R=0.1 ; $\nu_{th}(0)=0$
$E_k^2(t)$
10^{+2}
10^{+1}
10^{0}
10^{-1}
10^{-2}
n=4
n=3
n=4
n=5
n=1
n=2
n=3
n=1
n=2
n=5
$k=0.05\ n$
t →
0 1 2 3 4 5 6 7 8 9 10 11 12 13 14

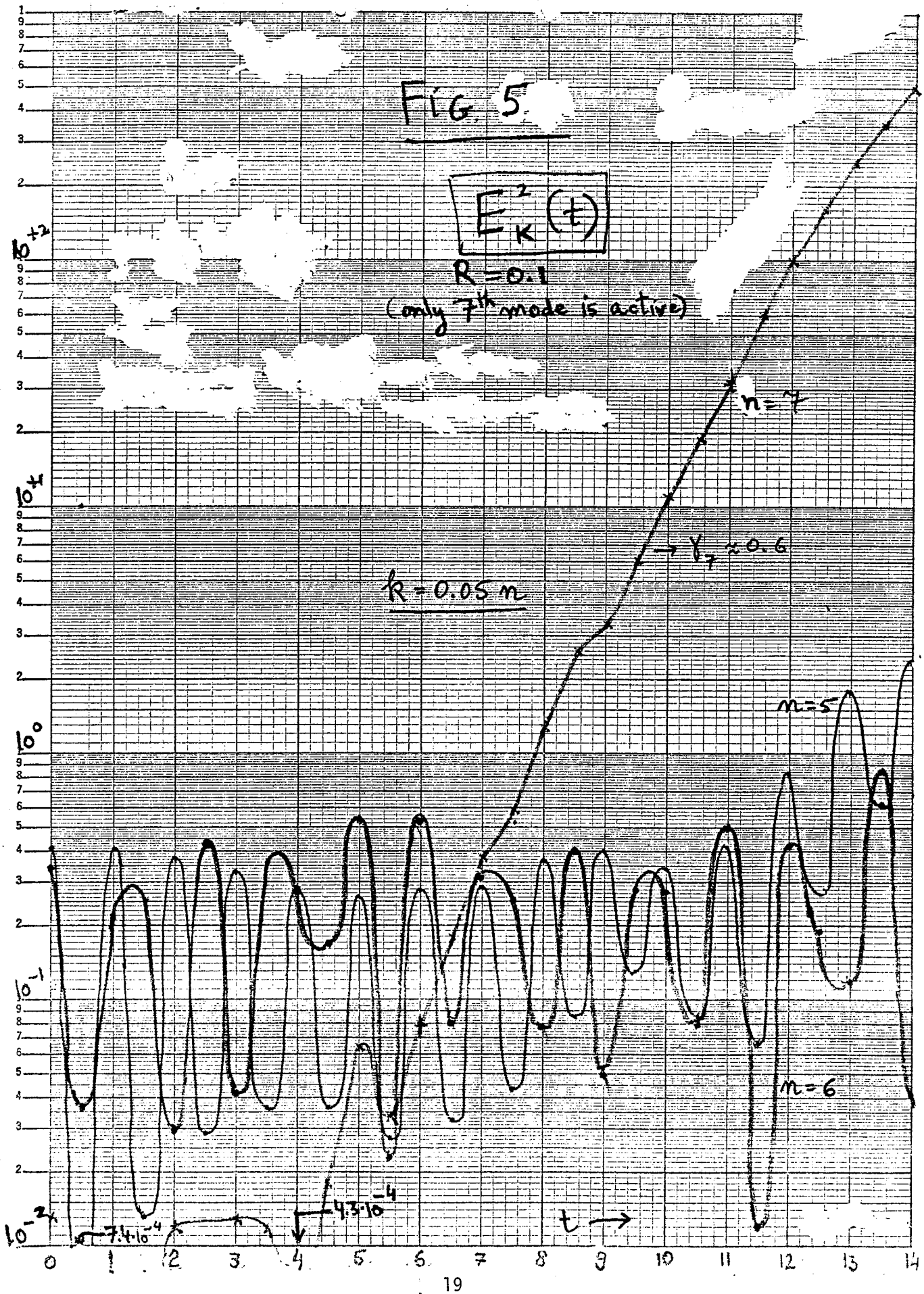
FIG. 5
$E_K^2(t)$
R = 0.1
(only 7th mode is active)
n = 7
$\gamma_7 \approx 0.6$
R = 0.05 n
n = 5
n = 6
10^{+2}
10^{+1}
10^{0}
10^{-1}
10^{-2}
$7.4 \cdot 10^{-4}$
$4.3 \cdot 10^{-4}$
t →
0 1 2 3 4 5 6 7 8 9 10 11 12 13 14

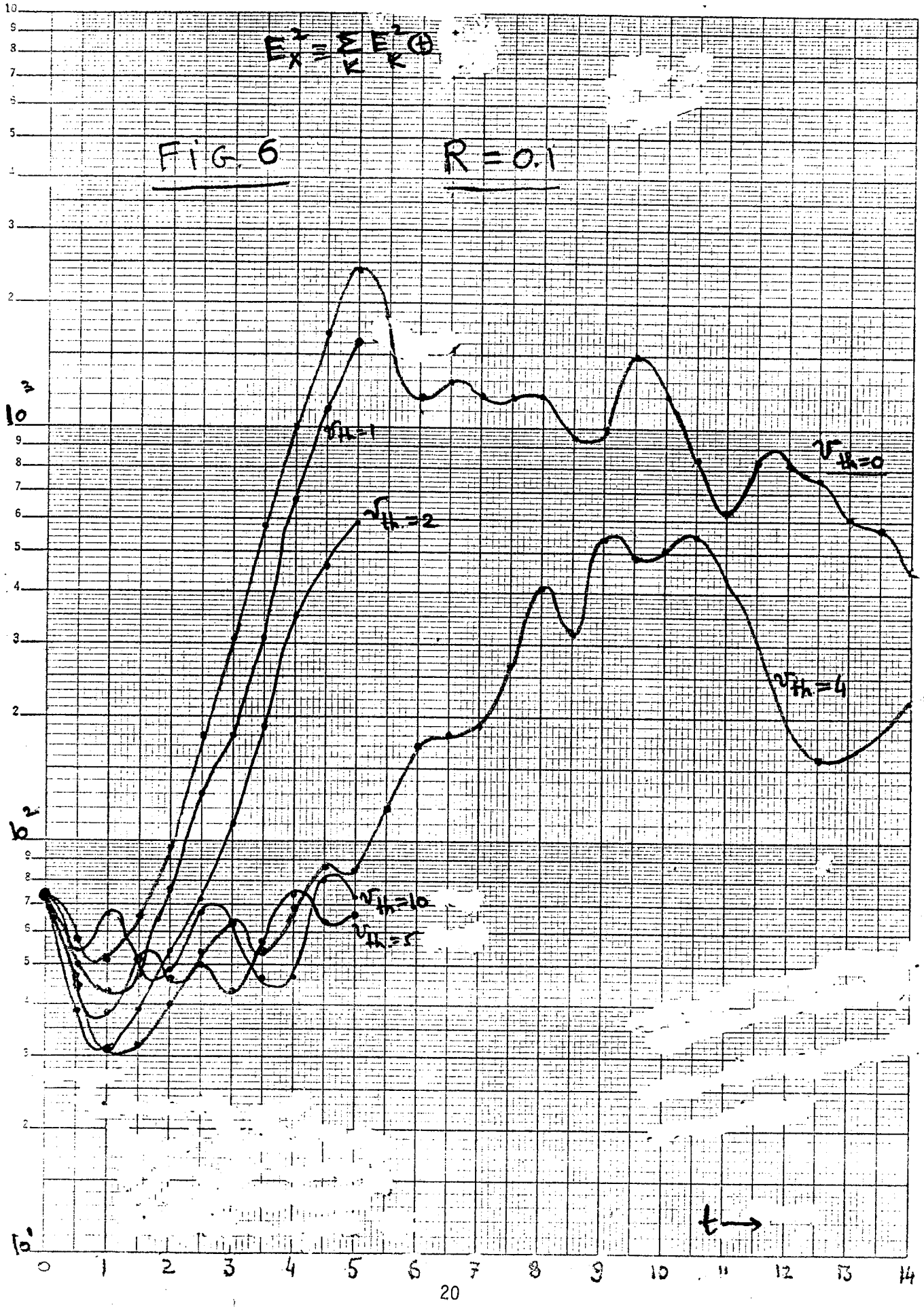

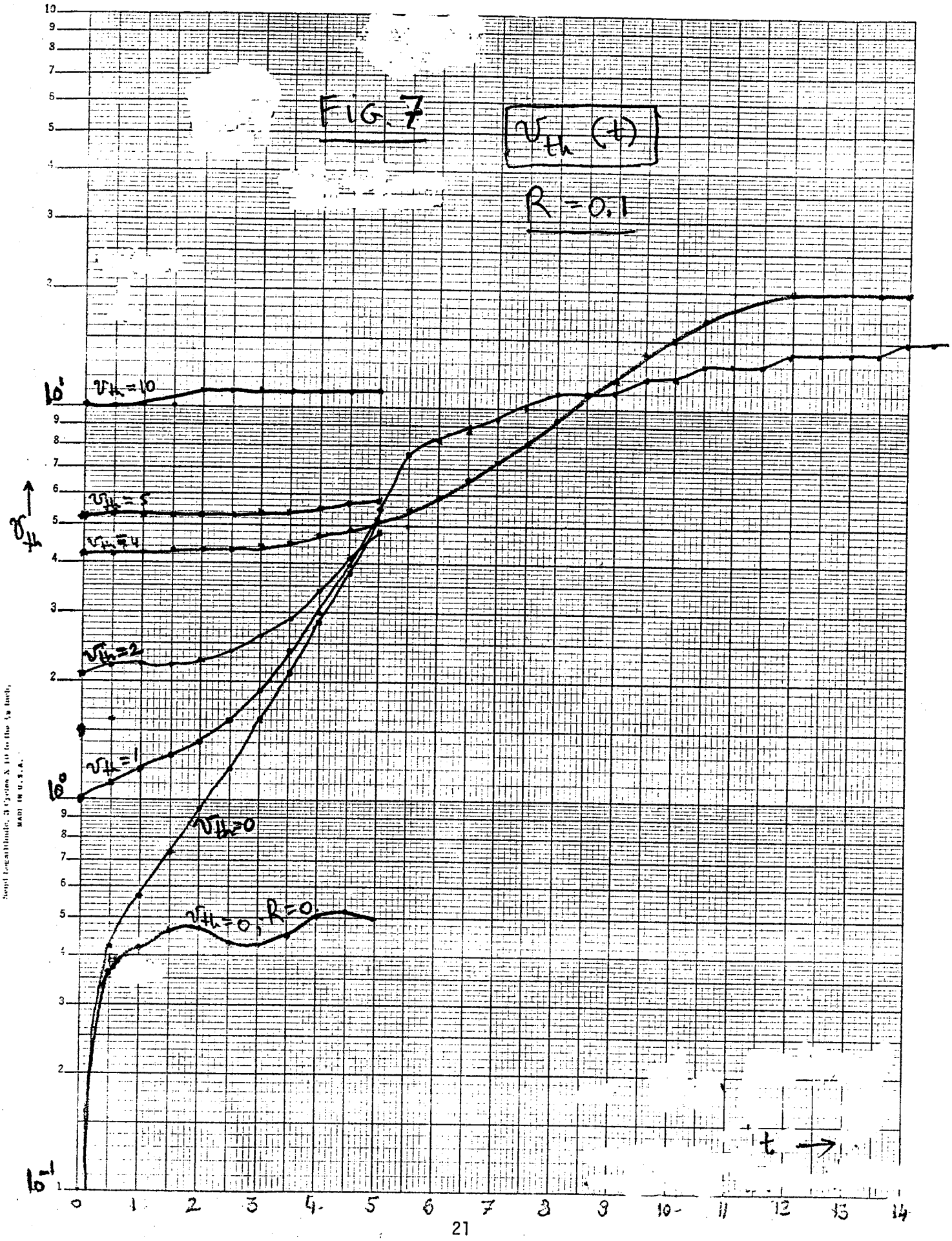

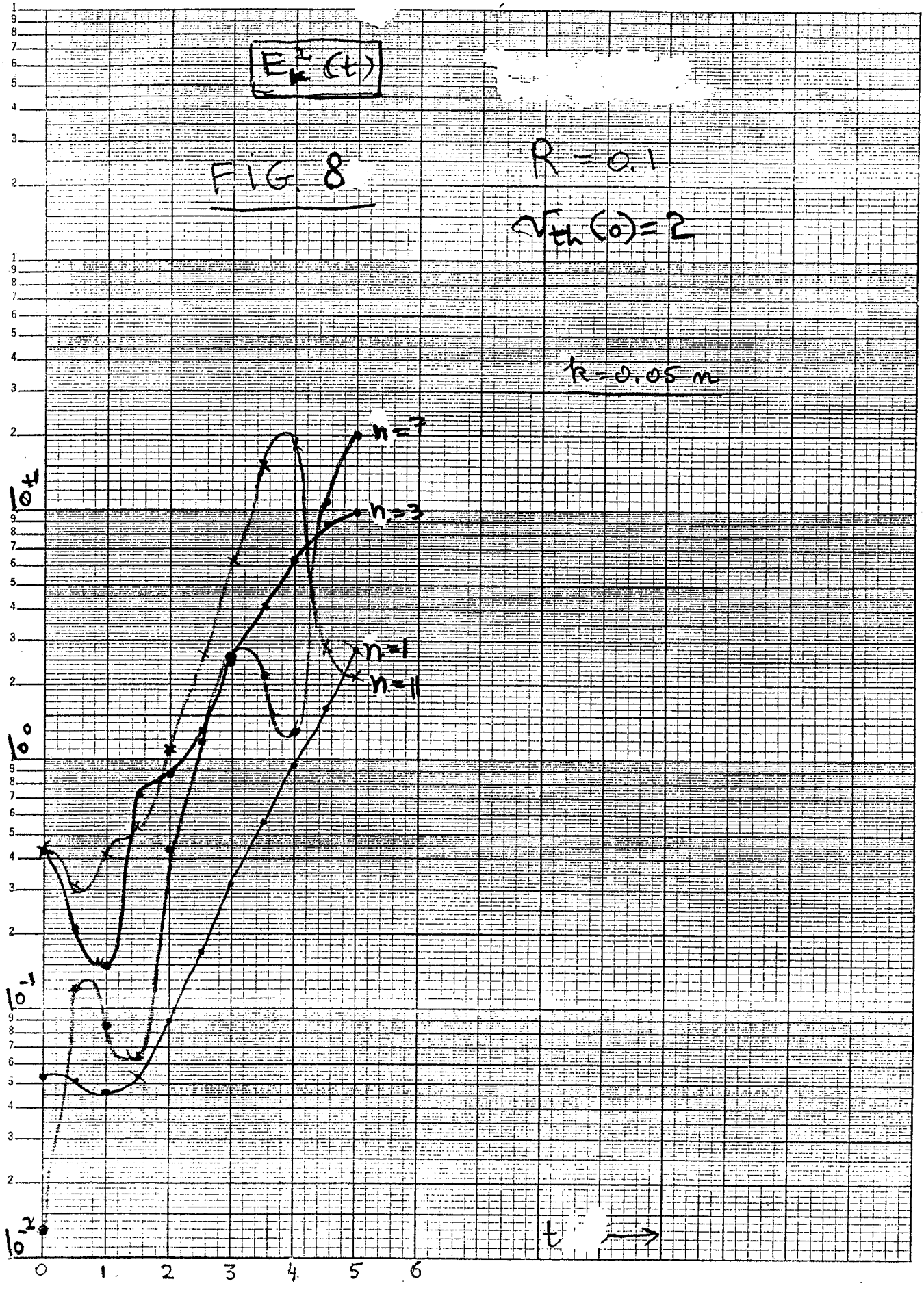
$E_k^2(t)$
FIG. 8
R = 0.1
$\sqrt{T_{th}}(0) = 2$
k = 0.05 m
n = 7
n = 3
n = 1
n = 11
10^{+1}
10^{0}
10^{-1}
10^{-2}
t
0
1
2
3
4
5
6

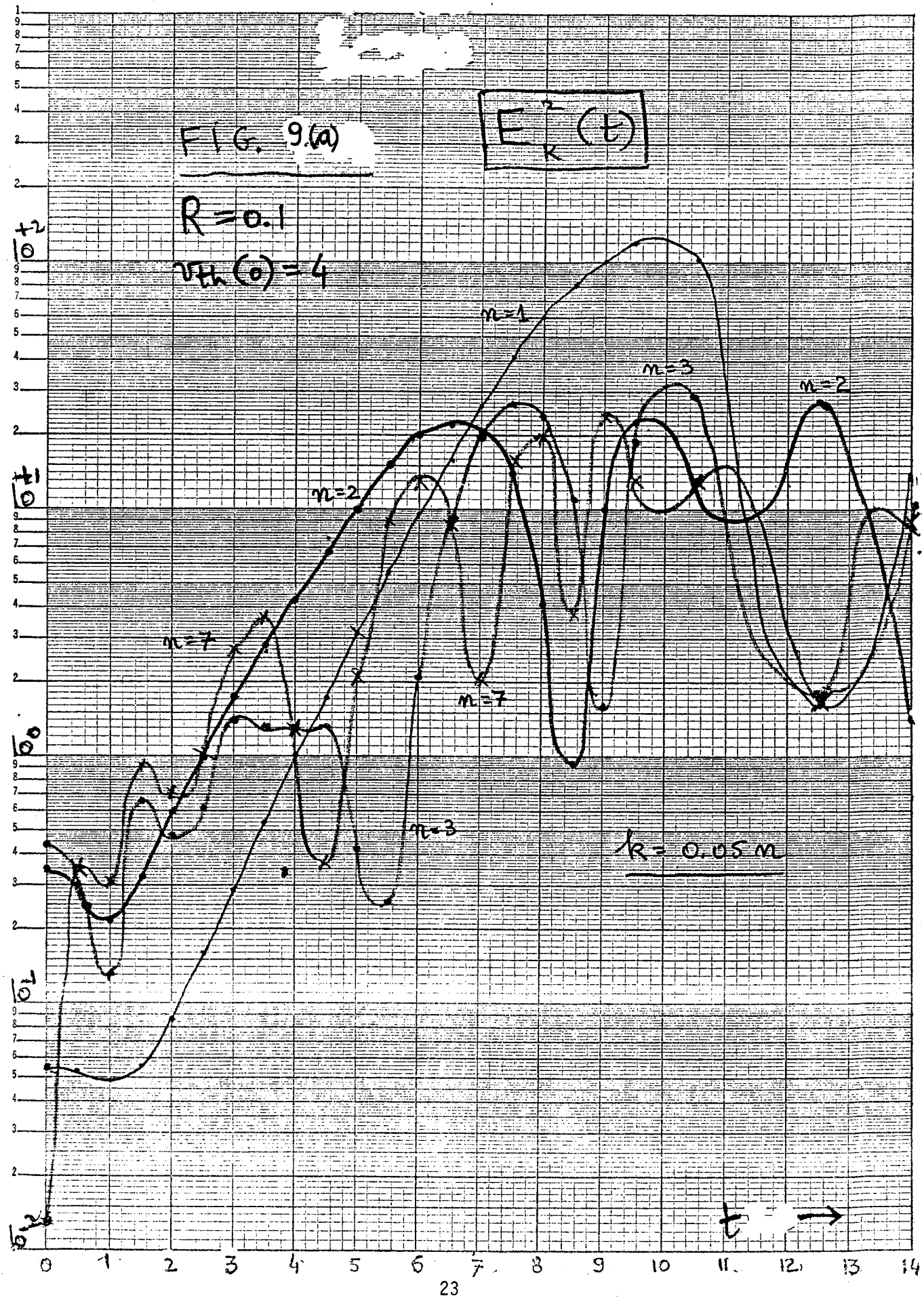
FIG. 9.(a)
$E_K^2(t)$
R = 0.1
$v_{th}(0) = 4$
n=1
n=3
n=2
n=2
n=7
n=7
n=3
R = 0.05 m
t →
+2
+1
0
-1
-2
0 1 2 3 4 5 6 7 8 9 10 11 12 13 14

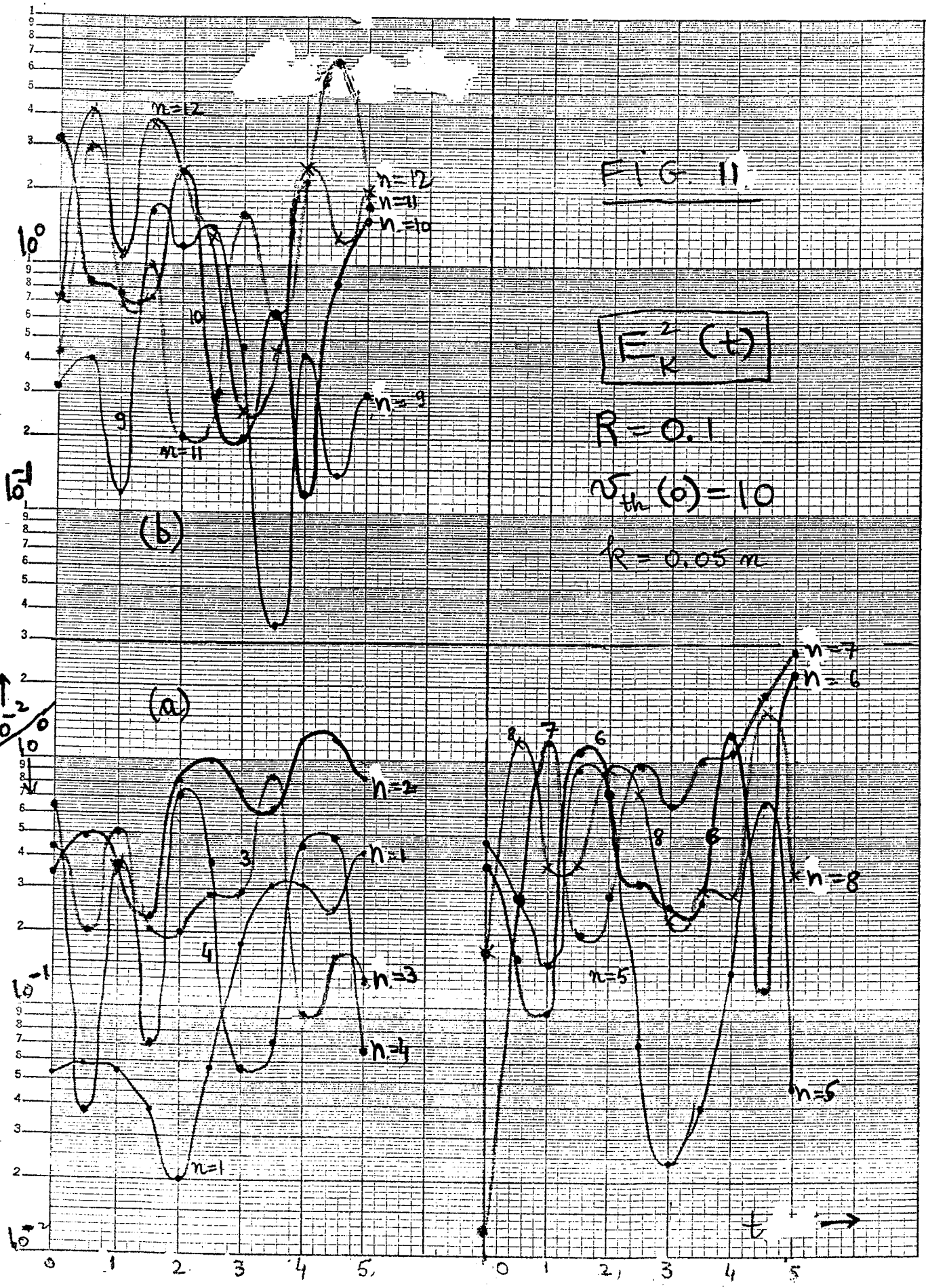
FIG. 11
$|E_R^2(t)|$
R = 0.1
$v_{th}(0) = 10$
R = 0.05 m
(a)
(b)
n=12
n=11
n=10
n=9
n=11
n=2
n=1
n=3
n=4
n=1
n=7
n=6
n=8
n=5
n=5
t →